OPTI 2014
An International Conference on
Engineering and Applied Sciences Optimization
M. Papadrakakis, M.G. Karlaftis, N.D. Lagaros (eds.)
Kos Island, Greece, 4-6, June 2014

# ON THE USE OF SYNCHRONOUS AND ASYNCHRONOUS SINGLE-OBJECTIVE DETERMINISTIC PARTICLE SWARM OPTIMIZATION IN SHIP DESIGN PROBLEMS

**A. Serani[1,2], M. Diez[1], C. Leotardi[1], D. Peri[3], G. Fasano[4], U. Iemma[2], E.F. Campana[1]**

[1]National Research Council–Marine Technology Research Institute (CNR-INSEAN)
Via di Vallerano 139, 00128 Rome, Italy
e-mail: {matteo.diez, emiliofortunato.campana}@cnr.it; c.leotardi@insean.it

[2]Department of Engineering, Roma Tre University
Via Vito Volterra 62, 00146 Rome, Italy
e-mail: {andrea.serani, umberto.iemma}@uniroma3.it

[3]National Research Council–Institute for Applied Mathematics "Mauro Picone" (CNR-IAC)
Via dei Taurini 19, 00185 Rome, Italy
e-mail: d.peri@iac.cnr.it

[4]Department of Management, Ca' Foscari University of Venice
San Giobbe, Cannaregio 873, 30121 Venice, Italy
e-mail: fasano@unive.it

**Keywords:** Simulation-based design, derivative-free optimization, global optimization, PSO.

**Abstract.** *A guideline for an effective and efficient use of a deterministic variant of the Particle Swarm Optimization (PSO) algorithm is presented and discussed, assuming limited computational resources. PSO was introduced in Kennedy and Eberhart (1995) and successfully applied in many fields of engineering optimization for its ease of use. Its performance depends on three main characteristics: the number of swarm particles used, their initialization in terms of initial location and speed, and the set of coefficients defining the behavior of the swarm. Original PSO makes use of random coefficients to sustain the variety of the swarm dynamics, and requires extensive numerical campaigns to achieve statistically convergent results. Such an approach can be too expensive in industrial applications, especially when CFD simulations are used, and for this reason, efficient deterministic approaches have been developed (Campana* et al. *2009). Additionally, the availability of parallel architectures has offered the opportunity to develop and compare synchronous and asynchronous implementation of PSO. The objective of present work is the identification of the most promising implementation for deterministic PSO. A parametric analysis is conducted using 60 analytical test functions and three different performance criteria, varying the number of particles, the initialization of the swarm, and the set of coefficients. The most promising PSO setup is applied to a ship design optimization problem, namely the high-speed Delft catamaran advancing in calm water at fixed speed, using a potential-flow code.*

## 1 INTRODUCTION

Particle Swarm Optimization (PSO) was originally introduced by Kennedy and Eberhart [1, 2], based on the social-behavior metaphor of a flock of birds or a swarm of bees in search for food, and belongs to the class of heuristic algorithms for single-objective evolutionary derivative-free global optimization. Derivative-free global optimization approaches are usually preferred to derivative-based local approaches, when objectives are noisy, derivatives are unknown and the existence of multiple local optima cannot be excluded, as often encountered in simulation-based design (SBD) optimization. Original PSO makes use of random coefficients to sustain the variety of the swarm dynamics, and therefore requires extensive numerical campaigns to provide statistically convergent results. Such an approach can be too expensive in SBD optimization for industrial applications, when CPU-time expensive computer simulations are used directly as analysis tools. For these reason, efficient deterministic approaches (D-PSO) have been developed and their use in ship hydrodynamics applications has been proven to be effective and efficient, compared to local methods [3] and random PSO [4]. Moreover, the availability of parallel architectures and high performance computing (HPC) systems has offered the opportunity to extend original *synchronous* PSO (S-PSO) to CPU-time efficient *asynchronous* approaches (A-PSO) [5, 6]. Recent applications of PSO to ship SBD include medium- to high-fidelity hull-form and waterjet design optimization of fast catamaran, by morphing techniques [7, 8] and geometry modifications based on Karhunen-Loève expansion (KLE) [4], and low- to medium-fidelity optimization of unconventional multi-hull configurations [9]. When global techniques are used with CPU-time expensive solvers, the optimization process is computationally very expensive and its effectiveness and efficiency remain an algorithmic and technological challenge.

Effectiveness and efficiency of PSO are significantly influenced by the choice of three main parameters: (a) the number of swarm particles interacting during the evolutionary optimization, (b) the initialization of the particles in terms of initial location and speed, and (c) the set of coefficients defining the personal or social tendency of the swarm dynamics. These parameters and their effects on PSO have been studied by a number of authors (see, e.g., [10]). Nevertheless, a specific indication of the optimal number of particles to be used with PSO is not present, the particles initialization has been little discussed (although significantly affects the PSO algorithm performance), and the coefficient set has been rarely investigated in a systematic way, including exhaustive combination of all parameters.

The objective of the present work is the identification of the most effective and efficient parameters for S/A D-PSO, for use in SBD optimization. The focus is on industrial problems directly using CPU-time expensive analyses, with a number of design variables ranging from two to twenty and simulations budget up to 1024 times the number of variables.

The approach includes a parametric analysis using 60 analytical test functions [11, 12] characterized by different degrees of non-linearities and number of local minima, with full-factorial combination of: (a) number of particles, using power of two per number of design variables; (b) initialization of the swarm, in terms of initial position and velocity, by Hammersley distributions [13]; (c) five set of coefficients, chosen from literature [14, 15, 16, 17, 18, 19]. Box constraints are treated by an inelastic-wall-type approach (IW) [20]. Three absolute metrics are defined and applied for the evaluation of the algorithm performances, based on the distance between PSO-found and analytical optima. The most significant parameter among (a), (b) and (c) is identified, based on the associated relative variability of the results. The most promising parameters for S/A D-PSO are defined and applied to an industrial problem, namely a fast catamaran hull-form

optimization in calm water at fixed speed. The objective function is the total resistance over displacement ratio. The hull geometry modification is performed using the KLE-based morphing approach presented in [4], using respectively four- and six-dimensional design spaces. Inelastic and semi-elastic wall-type (IW/SEW) approaches are used for box constraints. Computer simulations are performed using a potential flow (PF) model with the INSEAN-WARP code [21]. Finally, present optimization results are compared with those obtained in earlier research, based on a high-fidelity URANS solver [4].

## 2 PSO FORMULATIONS

Consider an *objective function*:

$$f(x) \;:\; \mathbb{R}^n \longrightarrow \mathbb{R} \tag{1}$$

The global optimization problem reads as follows

$$\min_{\mathbf{x}\in\mathcal{L}} f(\mathbf{x}), \quad \mathcal{L} \subset \mathbb{R}^n \tag{2}$$

where $\mathcal{L}$ is a closed and bounded set belonging to $\mathbb{R}^n$. To minimize the objective function $f$ is necessary to find $a \in \mathcal{L}$ so that:

$$\forall\, b \in \mathcal{L} \;\; : \;\; f(a) \leq f(b) \tag{3}$$

Then $a$ is a global minimum for the function $f(\mathbf{x})$. Usually, the identification of the global minimum is not possible or very hard, therefore solutions with sufficient good fitness are considered acceptable for practical purposes. In PSO, candidate solutions are the particles, denoted by $\mathbf{x} \in \mathcal{L}$ with associated fitness $f(\mathbf{x})$.

### 2.1 Original formulation

The original formulation of the PSO algorithm, as presented by Shi and Eberhart [14], is

$$\begin{cases} \mathbf{v}_i^{k+1} = w\mathbf{v}_i^k + c_1 r_1(\mathbf{x}_{i,pb} - \mathbf{x}_i^k) + c_2 r_2(\mathbf{x}_{gb} - \mathbf{x}_i^k) \\ \mathbf{x}_i^{k+1} = \mathbf{x}_i^k + \mathbf{v}_i^{k+1} \end{cases} \tag{4}$$

The above equations represent speed and position of the *i*-th particle at the *k*-th iteration respectively: $w$ is the *inertia weight*; $c_1$ and $c_2$ are the social and cognitive learning rate; $r_1$ and $r_2$ are two random numbers in the range $[0, 1]$; $\mathbf{x}_{i,pb}$ is the *personal best* position ever found by the $i$-th particle and $\mathbf{x}_{gb}$ is *global best* position ever found among all particles.

From the work of Clerc, Kennedy, Eberhart and Shi [22, 23, 24, 25, 15] appears that use of a *constriction factor* $\chi$ may be necessary to ensure convergence of PSO. Accordingly, the system in Eq. 4 is amended as follows

$$\begin{cases} \mathbf{v}_i^{k+1} = \chi\left[\mathbf{v}_i^k + c_1 r_1(\mathbf{x}_{i,pb} - \mathbf{x}_i^k) + c_2 r_2(\mathbf{x}_{gb} - \mathbf{x}_i^k)\right] \\ \mathbf{x}_i^{k+1} = \mathbf{x}_i^k + \mathbf{v}_i^{k+1} \end{cases} \tag{5}$$

$$\chi = \frac{2}{\left|\sqrt{2-\varphi-\sqrt{\varphi^2-4\varphi}}\right|}, \;\; \text{where} \;\; \varphi = c_1 + c_2, \;\; \varphi > 4 \tag{6}$$

Typically, when Clerc's constriction method is used [23], $\varphi$ value is set to $4.1$, with $\chi = 0.729$, $c_1 = c_2 = 1.494$.

### 2.2 Deterministic formulation (D-PSO)

In order to make the overall PSO more efficient for use in SBD with CPU-time expensive analyses, a deterministic algorithm was formulated in [3] by suppressing the random coefficients in Eq. 5, which becomes

$$\begin{cases} \mathbf{v}_i^{k+1} = \chi \left[ \mathbf{v}_i^k + c_1(\mathbf{x}_{i,pb} - \mathbf{x}_i^k) + c_2(\mathbf{x}_{gb} - \mathbf{x}_i^k) \right] \\ \mathbf{x}_i^{k+1} = \mathbf{x}_i^k + \mathbf{v}_i^{k+1} \end{cases} \tag{7}$$

The above formulation was compared to the original random PSO in, e.g., [4].

### 2.3 Synchronous and asynchronous implementations (S/A-PSO)

The *synchronous* implementation of PSO updates personal and global bests, particles speed and position at the end of each iteration. If the evaluation time of the objective function is significantly not uniform (e.g., due to iterative process/convergence of analysis tools), this leads to an increase of wall-clock time and CPU-time reservation. S-PSO is presented as a pseudo-code in the following and as a block diagram in Fig. 1a.

**Algorithm 1** S-PSO

For $k = 1$, number of iterations
  For $i = 1$, number of particles
    Evaluate objective function $f(\mathbf{x}_i)$
  End
  Update $\mathbf{x}_{i,pb}$, $\mathbf{x}_{gb}$, and particle positions and velocities $\mathbf{x}_i^{k+1}$, $\mathbf{v}_i^{k+1}$
End

In contrast to S-PSO, the *asynchronous* implementation updates personal and global bests, particles speed and position as soon as the information is available and the individual particle accomplished its analysis and is ready for a new one. A-PSO is presented as a pseudo-code in the following and as a block diagram in Fig. 1b.

**Algorithm 2** A-PSO

For $k = 1$, number of iterations
  For $i = 1$, number of particles
    Evaluate objective function $f(\mathbf{x}_i)$
    Update $\mathbf{x}_{i,pb}$, $\mathbf{x}_{gb}$, and particle positions and velocities $\mathbf{x}_i^{k+1}$, $\mathbf{v}_i^{k+1}$
  End
End

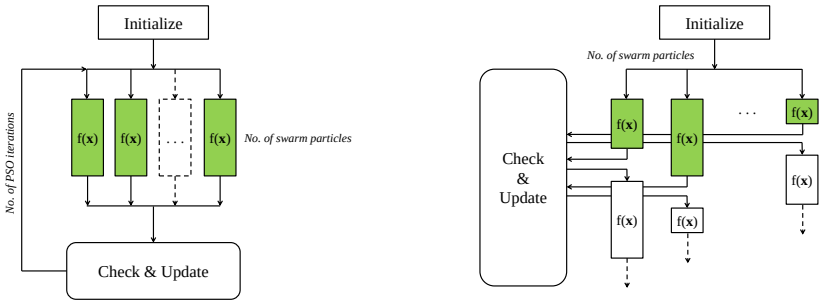


(a) Synchronous PSO (b) Asynchronous PSO

Figure 1: Block diagram for parallel PSO algorithm. The green boxes represent the first set of particles evaluated by the algorithm

### 2.4 Box constraints

The original PSO provides a *free* update of position and velocity of particles, regardless of the domain of interest and its bounds. This implies that, during the evolution of the swarm, the particles are allowed to go outside the domain bounds. This can be a critical issue in SBD problems, when the domain bounds cannot be violated due to physical/geometrical/grids constraints. Accordingly, a barrier (wall) is used on the bounds of the research space in order to confine the particles [26, 27]. Herein, the approach presented in [20] is used.

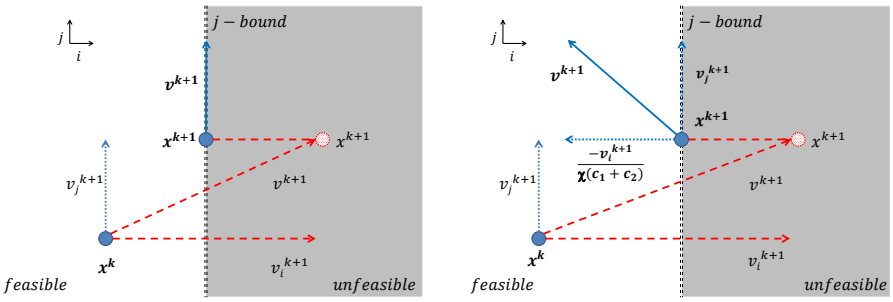


(a) Inelastic Wall (b) Semi-Elastic Wall

Figure 2: Inelastic (a) and semi-elastic (b) wall type approaches applied in the transition from $k$-th to $(k+1)$-th PSO iteration

The particles are confined with an *inelastic wall* (IW) type approach. Specifically, if a particle is found to exceed one of the bounds in the transition from $k$-th to $(k+1)$-th PSO iteration, it is placed on the bound setting to zero the associated velocity component (see Fig.2a). This approach helps the algorithm to explore the domain bounds. The IW approach is implemented herein as follows.

**Algorithm 3** Inelastic-wall-type approach (IW)

For $i = 1$, number of particles
  For $j = 1$, number of variables
    if $x_i^j > x_i^{j,max}$ then $x_i^j = x_i^{j,max}$, $v_i^j = 0$
    if $x_i^j < x_i^{j,min}$ then $x_i^j = x_i^{j,min}$, $v_i^j = 0$
  End
End

The use of IW has some limitation: in the unlikely event that all the particles tend to leave the domain from the same hyper-corner, the IW sets all speeds to zero and the PSO algorithm may stop. For this reason, a *semi-elastic wall* (SEW) type approach is also used. Accordingly, the particle is placed on the bound, while the associated velocity component is defined as follows (see also Fig. 2b):

**Algorithm 4** Semi-elastic-wall-type approach (SEW)

For $i = 1$, number of particles
  For $j = 1$, number of variables
    if $x_i^j > x_i^{j,max}$ then $x_i^j = x_i^{j,max}$, $v_i^j = -\frac{v_i^j}{\chi(c_1+c_2)}$
    if $x_i^j < x_i^{j,min}$ then $x_i^j = x_i^{j,min}$, $v_i^j = -\frac{v_i^j}{\chi(c_1+c_2)}$
  End
End

The damping factor $[\chi(c_1 + c_2)]^{-1}$ is used to ensure that the particle falls within the feasible domain.

## 3 PSO PARAMETERS AND EVALUATION METRIC

PSO parameters used are defined in the following. Their full-factorial combination is taken into account, resulting in 210 PSO setups.

### 3.1 Number of particles

The number of particles used is defined as

$$N_p = 2^m \cdot N_{dv}\,, \qquad \text{with} \qquad m \in \mathbb{N}\,[1, 7] \tag{8}$$

therefore ranging from $2 \cdot N_{dv}$ to $128 \cdot N_{dv}$.

### 3.2 Particles initialization

The initialization of particles location and speed is performed using a deterministic and homogeneous distribution, following the Hammersley sequence sampling [13]. Specifically, let $\mathbf{p} = \{p_1, \ldots, p_{N_{dv}-1}\}$ be a vector of prime numbers with $p_i \neq p_j, \forall i \neq j$. Any positive integer $i$ can be expressed using any $p_j$ by

$$i = \sum_{k=0}^{r} a_k p_j^k \tag{9}$$

where $r$ is a suitable integer and $a_k$ is an integer in $[0, p_j - 1]$. Finally, define $\phi_{p_j}(i) = \sum_{k=0}^{r} a_k / p_j^{k+1}$ and the $i$-th particle location as

$$\zeta_i = \left\{ \frac{i}{N_p},\, \phi_{p_1}(i),\, \cdots,\, \phi_{p_{N_{dv}-1}}(i) \right\} \quad \text{for } \; i = 0, 1, 2, ..., N_p - 1 \tag{10}$$

The above equation is applied to three different regions, defined as:

1. entire optimization domain (red dots in Fig. 3a)
2. domain bounds (blu triangles in Fig. 3b)
3. domain and bounds (red dots and blue triangles in Fig. 3c)

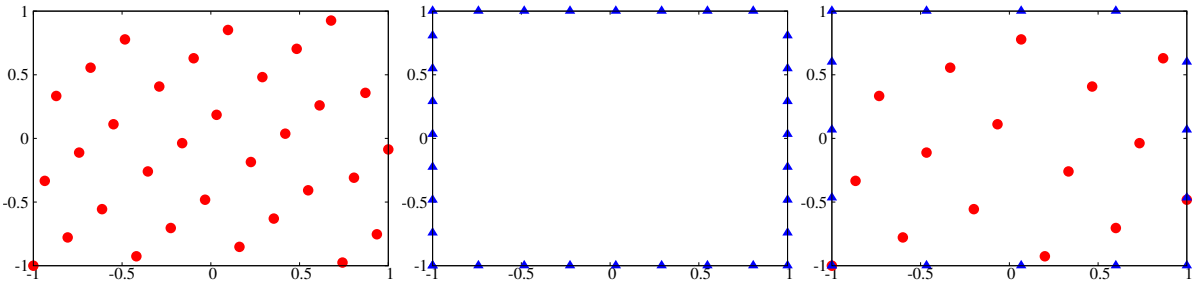

(a) Domain (b) Bounds (c) Domain and bounds

Figure 3: Examples of initializations in $\mathcal{L} = [-1, 1] \times [-1, 1]$ with 32 particles

The initial velocity is defined by the following positions:

- null velocity:

$$\mathbf{v}_i = 0, \;\; \forall\, i \in [1,\, N_p] \tag{11}$$

- non-null velocity, based on initial particle position:

$$\mathbf{v}_i = \frac{2}{\sqrt{N_{dv}}} \left( \mathbf{x}_i - \frac{\mathbf{l} + \mathbf{u}}{2} \right) \tag{12}$$

where $\mathbf{l}$ and $\mathbf{u}$ represent the lower and upper bound for $\mathbf{x}$, respectively [4].

Combining initial position and velocity approaches results in six different initializations, summarized in Tab. 1.

Table 1: Swarm initialization

| **Hammersley, over** | $\mathbf{v} = 0$ | $\mathbf{v} \neq 0$ |
|---|---|---|
| Domain | A.0 | A.1 |
| Bounds | B.0 | B.1 |
| Domain and bounds | C.0 | C.1 |

### 3.3 Coefficient set

Table 2 summarizes the coefficient sets used herein. The first set is the original proposed by Eberhart and Clerc [14, 15]; the second was suggested by Carlisle and Dozier in [16]; the third is that proposed by Trela in [17]; the fourth is a further suggestion by Clerc in [18]; the fifth was suggested by Peri and Tinti in [19].

Table 2: Coefficient set

| **ID Set** | **Name** | $\chi$ | $c_1$ | $c_2$ | $\beta$ |
|---|---|---|---|---|---|
| 1 | Eberhart and Clerc (2000) | 0.729 | 2.050 | 2.050 | 0.869 |
| 2 | Carlisle and Dozier (2001) | 0.729 | 2.300 | 1.800 | 0.869 |
| 3 | Trelea (2003) | 0.600 | 1.700 | 1.700 | 0.642 |
| 4 | Clerc (2006) | 0.721 | 1.655 | 1.655 | 0.697 |
| 5 | Peri and Tinti (2012) | 0.754 | 2.837 | 1.597 | 0.953 |

As shown in [12], the particles free dynamics is oscillatory and stable if the following condition holds:

$$\begin{cases} 0 < a < 1 \\ \left(1 - \sqrt{a}\right)^2 < \omega < \left(1 + \sqrt{a}\right)^2 \end{cases} \tag{13}$$

where $a = \chi$ and $\omega = \chi\,(c_1 + c_2)$. Introducing

$$\beta = \frac{\omega - \left(1 - \sqrt{a}\right)^2}{\left(1 + \sqrt{a}\right)^2 - \left(1 - \sqrt{a}\right)^2} \tag{14}$$

the condition of Eq. 13 reduces to

$$\begin{cases} 0 < \chi < 1 \\ 0 < \beta < 1 \end{cases} \tag{15}$$

which is satisfied by all coefficient sets in Tab. 2.

### 3.4 Number of function evaluations and PSO iterations

The number of function evaluations $N_{feval}$ (evaluations budget) is defined as

$$N_{feval} = 2^n \cdot N_{dv}, \quad \text{where} \quad n \in \mathbb{N}\,[7, 10] \tag{16}$$

and therefore ranges from $128 \cdot N_{dv}$ to $1024 \cdot N_{dv}$. As per Eq. 8, the number of PSO iterations $N_{iter}$ is

$$N_{iter} = \frac{N_{feval}}{N_p} = \frac{2^n \cdot N_{dv}}{2^m \cdot N_{dv}} = 2^{n-m} \tag{17}$$

### 3.5 Evaluation metric

Three absolute performance criteria are introduced as evaluation metric, and defined as follows:

$$\Delta_x = \sqrt{\frac{1}{N_{dv}} \sum_{i=1}^{N_{dv}} \left( \frac{x_i - x_i^\star}{R_i} \right)^2} \qquad \Delta_f = \frac{f_{\min} - f^\star_{\min}}{f^\star_{\max} - f^\star_{\min}} \qquad \Delta = \sqrt{\frac{\Delta_x^2 + \Delta_f^2}{2}} \tag{18}$$

$\Delta_x$ is the root mean square of the normalized Euclidean distance (in the domain space) between PSO-found ($\mathbf{x}$) and analytical minimum ($\mathbf{x}^\star$); $R_i$ is the range of the $i$-th variable; $\Delta_f$ is the associated normalized distance in the image space, where $f_{\min}$ is the PSO-found minimum and $f^\star_{\min}$ is the analytical one, and $f^\star_{\max}$ is the analytical maximum in the research space.

## 4 OPTIMIZATION PROBLEMS

### 4.1 Test functions

Sixty analytical test functions are used, as summarized in appendix A, Tab. 9. They include simple unimodal, highly complex multimodal and not differentiable problems (see e.g., [11, 12, 28]), with dimensionality ranging from two to twenty.

### 4.2 Hull-form SBD optimization of a high-speed catamaran

The high-speed Delft catamaran [7] is used as SBD test problem. The objective function is the total resistance over displacement ratio ($obj = R_t/\delta$) in calm water, advancing at Froude number ($Fr$) equal to 0.5 [4]. Geometry modifications have to fit in a box, defined by maximum overall length, beam and draught. Two feasible design spaces are considered. The first includes overall dimension bounds, whereas the second includes overall dimension bounds and, in addition, constant length between perpendiculars ($L_{pp}$). Modifications of the parent hull are performed using high-dimensional free-form deformation (FFD) and 95%-confidence dimensionality reduction based on KLE. Accordingly, four variables are used for the first design space and six for the second, referred to in the following as $4D$ and $6D$ space, respectively. New designs $\mathbf{g}$ are produced as

$$\mathbf{g}(\mathbf{x}) = \left( 1 - \sum_{j=1}^{N_{dv}} x_j \right) \mathbf{g}_0 + \sum_{j=1}^{N_{dv}} x_j \, \mathbf{g}_j \tag{19}$$

where $-1 \leq x_j \leq 1, \forall j \in [1, N_{dv}]$ are the design variables; $N_{dv} = 4$ for the first feasible design space whereas equals 6 for the second; $\mathbf{g}_0$ is the original geometry and $\mathbf{g}_j$ are the geometries

associated to the design space principal directions, as provided by KLE for dimensionality reduction. For details, the reader is referred to [4].

Simulations are conducted using the WARP (WAve Resistance Program) code, developed at CNR-INSEAN. Wave resistance computations are based on linear potential flow theory and details of equations, numerical implementation and validation of the numerical solver are given in [21]. The frictional resistance is estimated using a flat-plate approximation, based on local Reynolds number [29]. Simulations are performed for the right demi-hull, since the problem is symmetrical with respect to the $xz$ plane. The problem is discretized as follows: $20 \times 1$ panels in the inner-upstream sub-domain, $20 \times 40$ in the outer-upstream, $20 \times 1$ on the inner-hull, $20 \times 40$ on the outer-hull, $80 \times 1$ in the inner-dowstream, $80 \times 2$ in the transom-downstream, $80 \times 40$ in the outer-downstream and $125 \times 50$ on the body surface (Fig. 4). Domain bounds are defined by $1\ L_{pp}$ in the upstream, $4\ L_{pp}$ in the downstream and $2\ L_{pp}$ in the side.

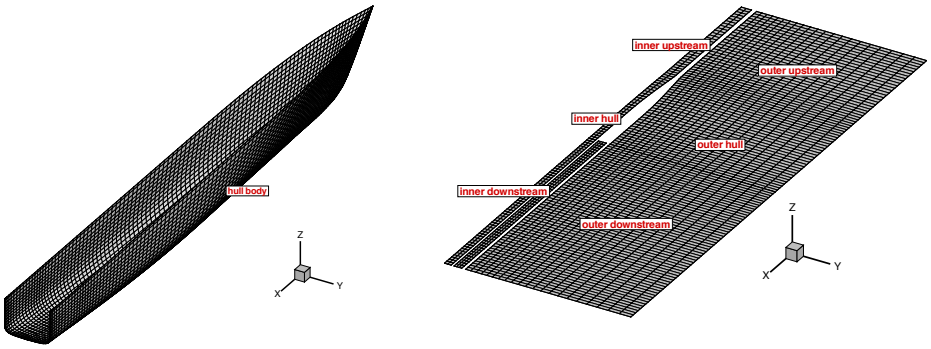


Figure 4: Panel-grid for INSEAN-WARP

## 5 NUMERICAL RESULTS

### 5.1 Test functions and guideline identification

Test-function results are presented in the following and used to define guidelines for S/A D-PSO.

#### 5.1.1 SD-PSO

Figures 5 and 6, show the performances of SD-PSO versus the budget of function evaluations, in terms of $\Delta_x$, $\Delta_f$, $\Delta$, for $N_{dv} < 10$ and $\geq 10$ respectively. Average values are presented, conditional to number of particles, particles initialization and coefficient set, respectively. Figures 7 and 8 show the relative variance $\sigma_r^2$ of $\Delta_x$, $\Delta_f$, $\Delta$ for $N_{dv} < 10$ and $\geq 10$ respectively, retained by each of the PSO parameters. The particles initialization is found the most significant parameters, especially for $N_{dv} \geq 10$, whereas the coefficient set is shown to be the least important. Tables 3 and 4 summarizes the five best performing setups based on $\Delta_x$, $\Delta_f$, $\Delta$, for $N_{dv} < 10$ and $\geq 10$ respectively, varying the budget of function evaluations available. Average values and standard deviations among all PSO setups are also provided.

### 5.1.2 AD-PSO

Generally, AD-PSO results are found similar to SD-PSO. Specifically, Figs. 9 and 10, show the performances of AD-PSO versus the budget of function evaluations, in terms of $\Delta_x$, $\Delta_f$, $\Delta$, for $N_{dv} < 10$ and $\geq 10$ respectively. Average values are presented, conditional to number of particles, particles initialization and coefficient set, respectively. Figures 11 and 12 show the relative variance $\sigma_r^2$ of $\Delta_x$, $\Delta_f$, $\Delta$ for $N_{dv} < 10$ and $\geq 10$ respectively, retained by each of the PSO parameters. The particles initialization is the most significant parameters, especially for low budgets and $N_{dv} \geq 10$. The coefficient set is shown to have a small effect on the performance, compared to other PSO parameters. Tables 5 and 6 summarizes the five best performing setups based on $\Delta_x$, $\Delta_f$, $\Delta$, for $N_{dv} < 10$ and $\geq 10$, respectively, varying the budget of function evaluations. Overall averages and standard deviations among all PSO setups are also included.

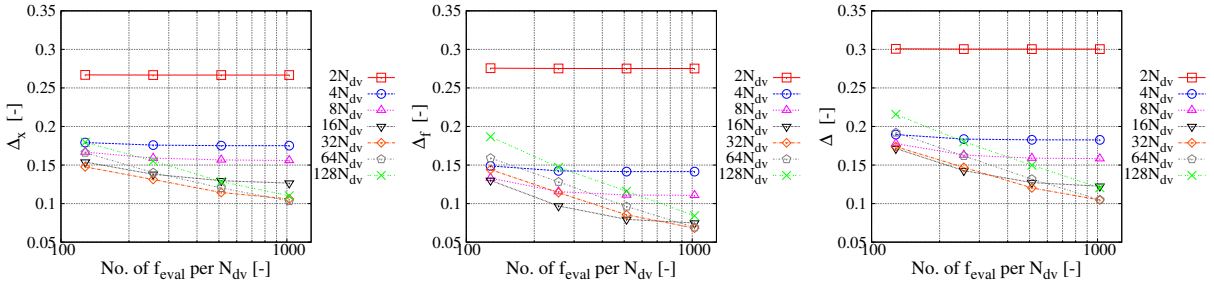


(a) Average performance, conditional to number of particles

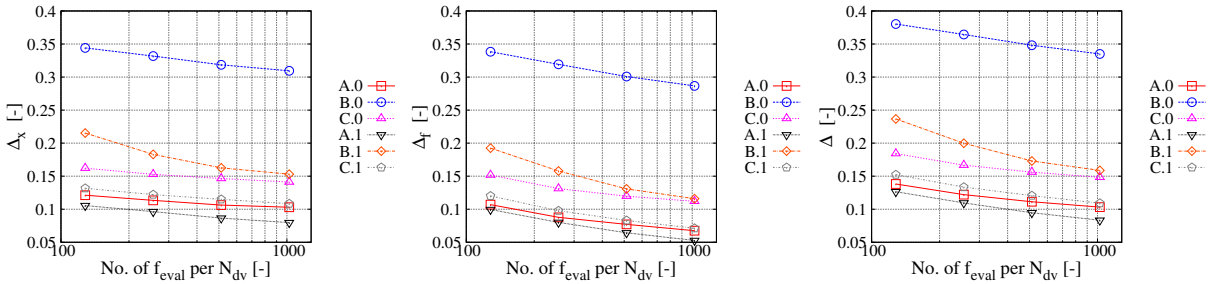


(b) Average performance, conditional to particle initialization

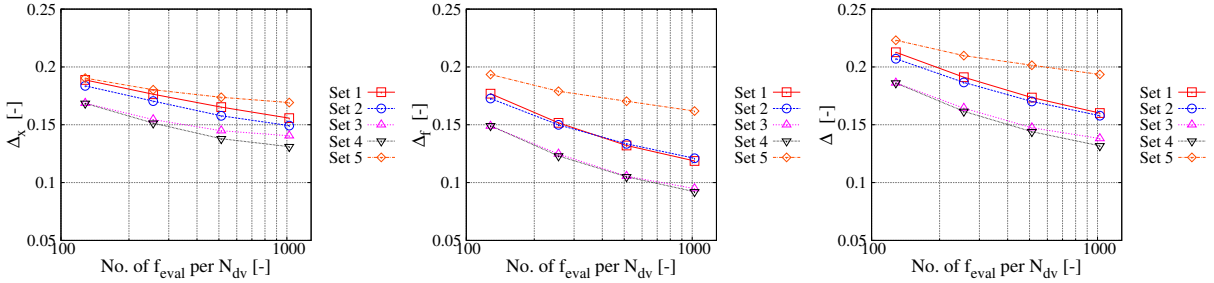


(c) Average performance, conditional to coefficient set

Figure 5: SD-PSO average performance for $N_{dv} < 10$

Table 3: Best performing setups for SD-PSO, $N_{dv} < 10$

| $N_{feval}/N_{dv}$ | Average (STD) | | | Best SD-PSO | | | | | | | | | | | |
|---|---|---|---|---|---|---|---|---|---|---|---|---|---|---|---|
| | $\Delta_x$ | $\Delta_f$ | $\Delta$ | $\frac{N_p}{N_{dv}}$ | Init | Coef | $\Delta_x$ | $\frac{N_p}{N_{dv}}$ | Init | Coef | $\Delta_f$ | $\frac{N_p}{N_{dv}}$ | Init | Coef | $\Delta$ |
| 128 | 0.180 (0.098) | 0.168 (0.114) | 0.203 (0.109) | 16 | A.1 | 3 | 0.072 | **4** | **C.1** | **4** | **0.015** | **4** | **C.1** | **4** | **0.064** |
| | | | | 64 | A.1 | 5 | 0.075 | 2 | A.1 | 4 | 0.030 | 2 | A.1 | 4 | 0.073 |
| | | | | 32 | A.1 | 3 | 0.076 | 8 | A.1 | 3 | 0.048 | 4 | C.1 | 3 | 0.083 |
| | | | | 16 | A.0 | 3 | 0.080 | 4 | A.1 | 3 | 0.053 | 16 | A.1 | 3 | 0.083 |
| | | | | 4 | C.1 | 3 | 0.080 | 4 | C.1 | 3 | 0.053 | 8 | A.1 | 3 | 0.087 |
| 256 | 0.166 (0.097) | 0.145 (0.118) | 0.183 (0.112) | 64 | A.1 | 4 | 0.063 | **4** | **C.1** | **4** | **0.014** | 16 | A.0 | 3 | 0.053 |
| | | | | 16 | A.1 | 3 | 0.064 | 16 | A.0 | 3 | 0.017 | 16 | A.1 | 3 | 0.055 |
| | | | | 32 | A.1 | 5 | 0.065 | 16 | A.1 | 3 | 0.026 | **4** | **C.1** | **4** | **0.060** |
| | | | | 16 | A.0 | 3 | 0.066 | 2 | A.1 | 4 | 0.030 | 2 | A.1 | 4 | 0.072 |
| | | | | 32 | C.0 | 3 | 0.067 | 8 | C.1 | 4 | 0.038 | 16 | A.0 | 4 | 0.053 |
| 512 | 0.156 (0.098) | 0.129 (0.120) | 0.167 (0.114) | 64 | A.1 | 4 | 0.049 | 16 | A.0 | 3 | 0.012 | 16 | C.0 | 3 | 0.049 |
| | | | | 64 | A.0 | 4 | 0.056 | **4** | **C.1** | **4** | **0.013** | 32 | A.1 | 3 | 0.049 |
| | | | | 64 | A.1 | 2 | 0.056 | 32 | C.0 | 3 | 0.017 | 32 | C.0 | 3 | 0.049 |
| | | | | 32 | A.1 | 5 | 0.058 | 16 | A.0 | 1 | 0.018 | 16 | A.1 | 3 | 0.053 |
| | | | | 32 | C.0 | 3 | 0.059 | 32 | A.1 | 3 | 0.019 | 16 | A.0 | 1 | 0.053 |
| 1024 | 0.149 (0.099) | 0.118 (0.123) | 0.156 (0.117) | 64 | A.1 | 4 | 0.038 | 64 | A.0 | 4 | 0.004 | 64 | A.1 | 4 | 0.030 |
| | | | | 64 | A.1 | 2 | 0.039 | 32 | C.1 | 4 | 0.005 | 64 | A.0 | 4 | 0.031 |
| | | | | 64 | A.0 | 4 | 0.043 | 64 | A.1 | 3 | 0.005 | 64 | A.1 | 3 | 0.039 |
| | | | | 128 | C.1 | 4 | 0.049 | 64 | A.0 | 3 | 0.007 | 64 | A.1 | 2 | 0.039 |
| | | | | 32 | A.1 | 1 | 0.049 | 64 | A.1 | 4 | 0.007 | 32 | C.1 | 4 | 0.041 |
| Av. | 0.163 (0.097) | 0.140 (0.118) | 0.177 (0.111) | 64 | A.1 | 4 | 0.047 | **4** | **C.1** | **4** | **0.014** | 16 | A.0 | 3 | 0.060 |
| | | | | 64 | A.0 | 4 | 0.062 | 16 | A.0 | 3 | 0.025 | **4** | **C.1** | **4** | **0.061** |
| | | | | 32 | A.1 | 5 | 0.064 | 2 | A.1 | 4 | 0.030 | 16 | A.1 | 3 | 0.061 |
| | | | | 16 | A.1 | 3 | 0.064 | 16 | A.1 | 3 | 0.034 | 32 | A.1 | 3 | 0.066 |
| | | | | 32 | A.1 | 3 | 0.065 | 32 | A.1 | 3 | 0.039 | 32 | C.0 | 3 | 0.071 |

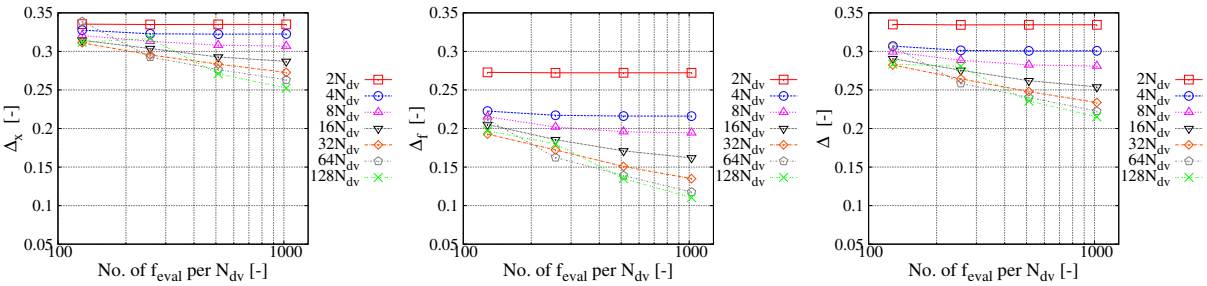


(a) Average performance, conditional to number of particles

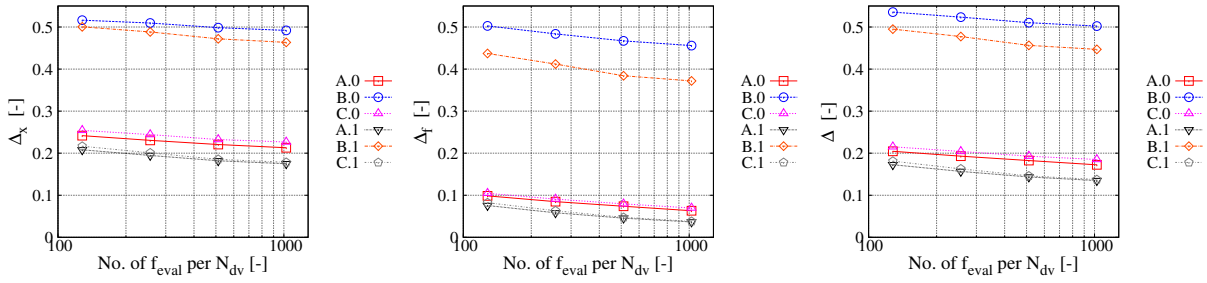


(b) Average performance, conditional to particle initialization

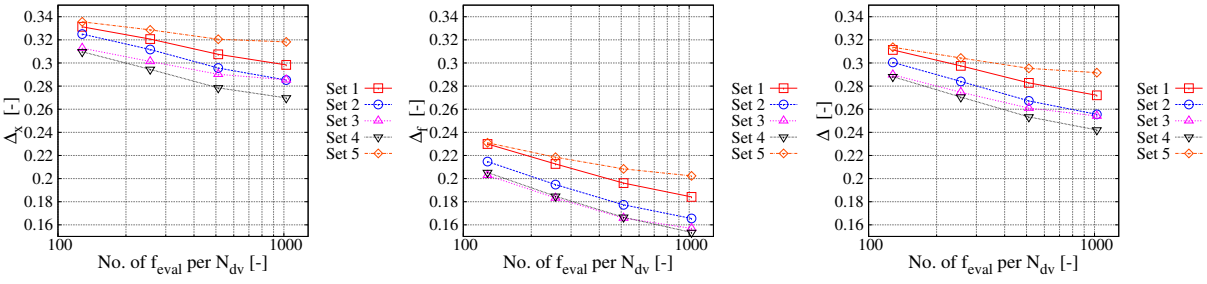


(c) Average performance, conditional to coefficient set

Figure 6: SD-PSO average performance for $N_{dv} \geq 10$

Table 4: Best performing setups for SD-PSO, $N_{dv} \geq 10$

| $N_{feval}/N_{dv}$ | Average (STD) | | | Best SD-PSO | | | | | | | | | | | |
|---|---|---|---|---|---|---|---|---|---|---|---|---|---|---|---|
| | $\Delta_x$ | $\Delta_f$ | $\Delta$ | $\frac{N_p}{N_{dv}}$ | Init | Coef | $\Delta_x$ | $\frac{N_p}{N_{dv}}$ | Init | Coef | $\Delta_f$ | $\frac{N_p}{N_{dv}}$ | Init | Coef | $\Delta$ |
| 128 | 0.323 | 0.217 | 0.301 | 2 | A.1 | 2 | 0.155 | 2 | C.1 | 2 | 0.023 | 2 | A.1 | 2 | 0.118 |
| | | | | 4 | A.1 | 4 | 0.155 | 2 | A.1 | 4 | 0.025 | 2 | C.1 | 2 | 0.119 |
| | | | | 2 | C.1 | 1 | 0.156 | 4 | C.1 | 2 | 0.027 | 2 | A.1 | 4 | 0.121 |
| | (0.136) | (0.195) | (0.162) | **4** | **C.1** | **4** | **0.158** | 4 | A.1 | 3 | 0.030 | **4** | **C.1** | **4** | **0.122** |
| | | | | 2 | A.1 | 4 | 0.159 | **4** | **C.1** | **4** | **0.031** | 4 | C.1 | 2 | 0.122 |
| 256 | 0.311 | 0.199 | 0.286 | 4 | C.1 | 2 | 0.149 | 4 | C.1 | 2 | 0.019 | 4 | C.1 | 2 | 0.108 |
| | | | | 4 | A.1 | 4 | 0.152 | 8 | A.1 | 4 | 0.019 | 8 | A.1 | 4 | 0.115 |
| | | | | 2 | A.1 | 2 | 0.153 | **4** | **C.1** | **4** | **0.021** | **4** | **C.1** | **4** | **0.116** |
| | (0.139) | (0.196) | (0.163) | 2 | C.1 | 1 | 0.154 | 8 | C.1 | 4 | 0.022 | 8 | C.1 | 4 | 0.116 |
| | | | | **4** | **C.1** | **4** | **0.156** | 2 | C.1 | 2 | 0.022 | 2 | A.1 | 2 | 0.117 |
| 512 | 0.298 | 0.183 | 0.272 | 4 | C.1 | 2 | 0.147 | 16 | A.1 | 3 | 0.011 | 4 | C.1 | 2 | 0.106 |
| | | | | 32 | A.1 | 4 | 0.149 | 8 | A.1 | 4 | 0.013 | 8 | C.1 | 4 | 0.110 |
| | | | | 4 | A.1 | 4 | 0.151 | 8 | C.1 | 2 | 0.014 | 8 | A.1 | 4 | 0.111 |
| | (0.140) | (0.197) | (0.165) | 64 | A.1 | 3 | 0.153 | 8 | A.0 | 4 | 0.017 | **4** | **C.1** | **4** | **0.114** |
| | | | | 8 | C.1 | 4 | 0.153 | 4 | C.1 | 2 | 0.018 | 8 | C.1 | 2 | 0.115 |
| 1024 | 0.291 | 0.172 | 0.263 | 32 | A.1 | 4 | 0.136 | 16 | A.1 | 3 | 0.009 | 32 | A.1 | 4 | 0.098 |
| | | | | 64 | A.1 | 3 | 0.144 | 16 | A.1 | 4 | 0.011 | 64 | A.1 | 3 | 0.105 |
| | | | | 64 | C.1 | 4 | 0.145 | 32 | A.1 | 4 | 0.011 | 4 | C.1 | 2 | 0.106 |
| | (0.142) | (0.199) | (0.168) | 4 | C.1 | 2 | 0.147 | 8 | A.1 | 4 | 0.012 | 16 | A.1 | 4 | 0.109 |
| | | | | 128 | A.1 | 4 | 0.148 | 32 | C.1 | 3 | 0.013 | 8 | C.1 | 4 | 0.109 |
| Av. | 0.306 | 0.193 | 0.280 | 4 | A.1 | 4 | 0.152 | 4 | C.1 | 2 | 0.020 | 4 | C.1 | 2 | 0.111 |
| | | | | 4 | C.1 | 2 | 0.152 | 8 | C.1 | 2 | 0.022 | **4** | **C.1** | **4** | **0.117** |
| | | | | 2 | A.1 | 2 | 0.153 | 2 | C.1 | 2 | 0.022 | 2 | A.1 | 2 | 0.117 |
| | (0.139) | (0.196) | (0.164) | 2 | C.1 | 1 | 0.154 | 8 | A.1 | 4 | 0.023 | 8 | C.1 | 4 | 0.117 |
| | | | | **4** | **C.1** | **4** | **0.156** | **4** | **C.1** | **4** | **0.039** | 2 | C.1 | 4 | 0.118 |

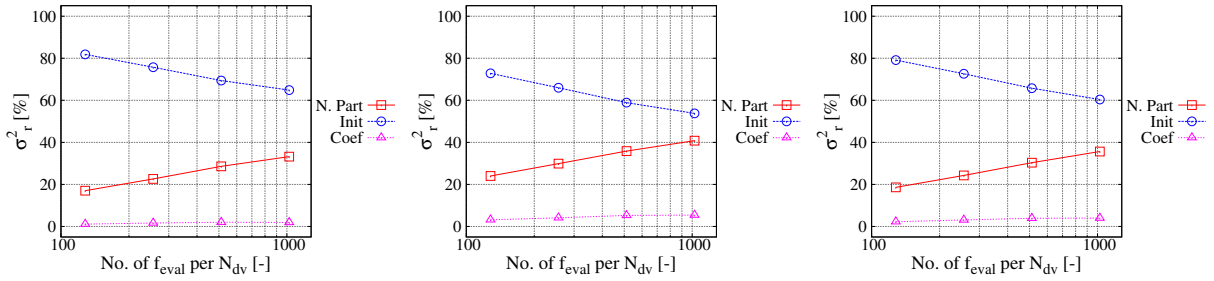


(a) $\Delta_x$ (b) $\Delta_f$ (c) $\Delta$

Figure 7: $\sigma_r^2(\%)$ of SD-PSO for $N_{dv} < 10$

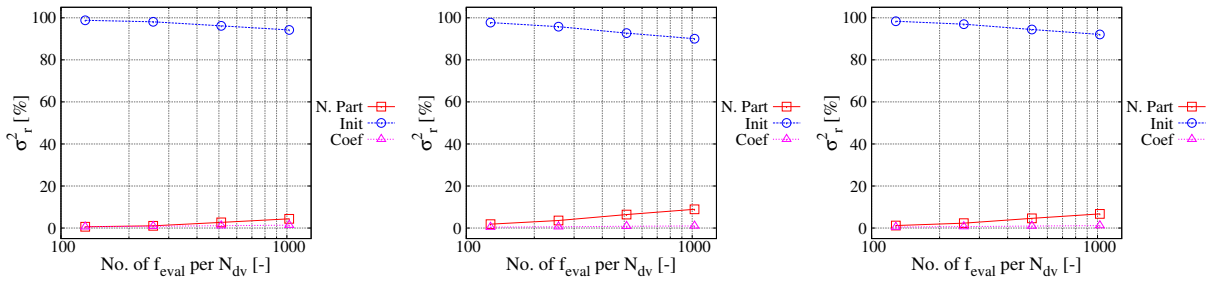


(a) $\Delta_x$ (b) $\Delta_f$ (c) $\Delta$

Figure 8: $\sigma_r^2(\%)$ of SD-PSO for $N_{dv} \geq 10$

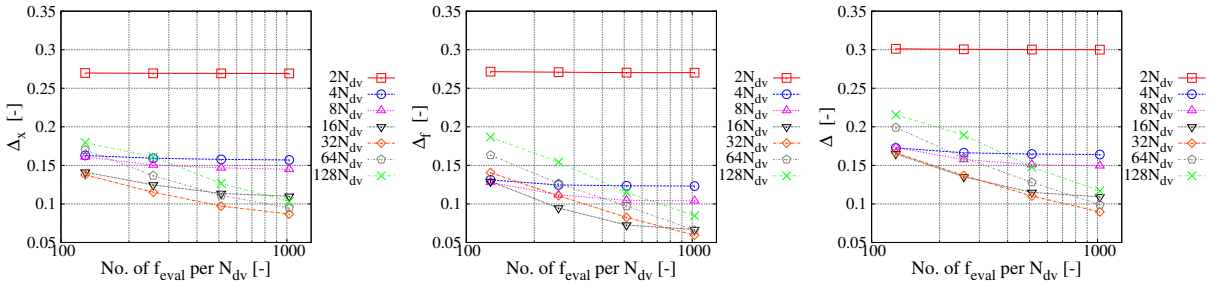


(a) Average performance, conditional to number of particles

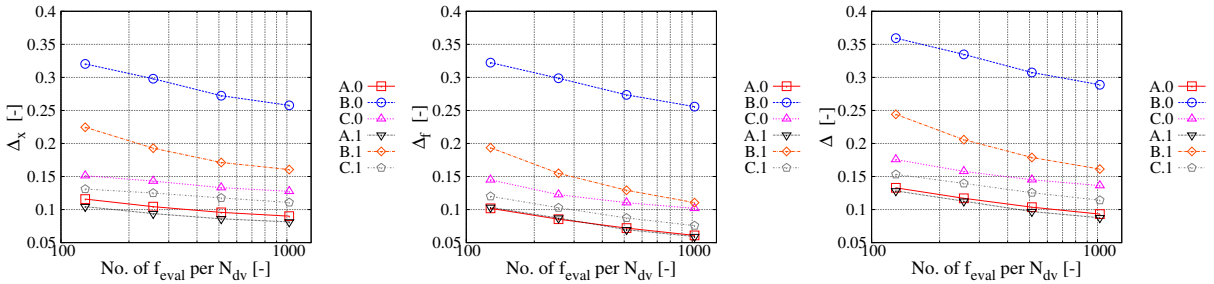


(b) Average performance, conditional to particle initialization

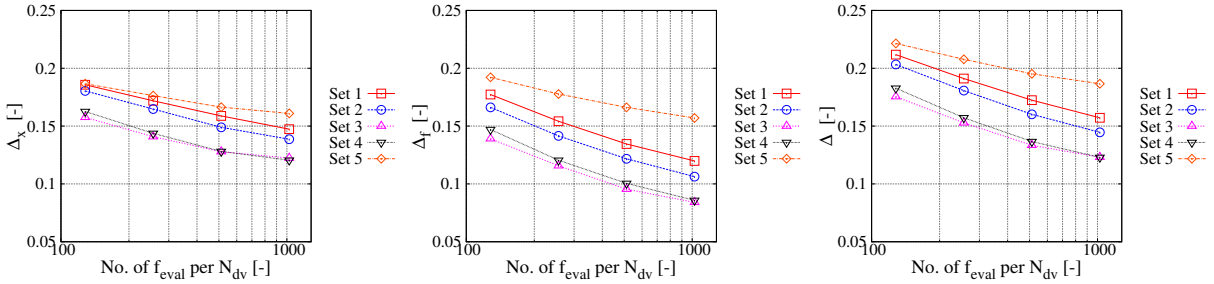


(c) Average performance, conditional to coefficient set

Figure 9: AD-PSO average performance for $N_{dv} < 10$

Table 5: Best performing setups for AD-PSO, $N_{dv} < 10$

| $N_{feval}/N_{dv}$ | Average (STD) | | | Best AD-PSO | | | | | | | | | | | |
|---|---|---|---|---|---|---|---|---|---|---|---|---|---|---|---|
| | $\Delta_x$ | $\Delta_f$ | $\Delta$ | $\frac{N_p}{N_{dv}}$ | Init | Coef | $\Delta_x$ | $\frac{N_p}{N_{dv}}$ | Init | Coef | $\Delta_f$ | $\frac{N_p}{N_{dv}}$ | Init | Coef | $\Delta$ |
| 128 | 0.175 | 0.164 | 0.199 | 16 | A.1 | 1 | 0.069 | 4 | C.1 | 3 | 0.004 | **4** | **C.1** | **4** | **0.053** |
| | | | | 16 | A.1 | 3 | 0.069 | **4** | **C.1** | **4** | **0.007** | 4 | C.1 | 3 | 0.061 |
| | | | | 16 | A.0 | 3 | 0.071 | 4 | C.0 | 3 | 0.021 | 4 | C.0 | 4 | 0.076 |
| | (0.096) | (0.113) | (0.107) | **4** | **C.1** | **4** | **0.073** | 4 | C.0 | 4 | 0.022 | 8 | A.1 | 3 | 0.080 |
| | | | | 16 | A.1 | 4 | 0.076 | 2 | A.1 | 4 | 0.037 | 2 | A.1 | 4 | 0.082 |
| 256 | 0.160 | 0.142 | 0.178 | 16 | A.1 | 2 | 0.057 | **4** | **C.1** | **4** | **0.003** | **4** | **C.1** | **4** | **0.046** |
| | | | | 16 | A.1 | 3 | 0.057 | 4 | C.1 | 3 | 0.004 | 4 | C.1 | 3 | 0.059 |
| | | | | 16 | A.1 | 1 | 0.059 | 4 | C.0 | 4 | 0.014 | 16 | A.0 | 3 | 0.066 |
| | (0.093) | (0.118) | (0.107) | 16 | A.0 | 3 | 0.060 | 4 | C.0 | 3 | 0.020 | 4 | C.0 | 4 | 0.067 |
| | | | | 16 | A.0 | 4 | 0.060 | 2 | A.1 | 4 | 0.037 | 16 | A.1 | 3 | 0.074 |
| 512 | 0.146 | 0.124 | 0.159 | 32 | C.1 | 4 | 0.046 | **4** | **C.1** | **4** | **0.003** | 16 | A.0 | 4 | 0.036 |
| | | | | 16 | A.0 | 4 | 0.049 | 4 | C.1 | 3 | 0.004 | **4** | **C.1** | **4** | **0.040** |
| | | | | 16 | A.1 | 2 | 0.050 | 16 | A.0 | 4 | 0.005 | 16 | A.1 | 2 | 0.053 |
| | (0.092) | (0.117) | (0.109) | 32 | A.1 | 4 | 0.051 | 4 | C.0 | 4 | 0.014 | 16 | A.1 | 3 | 0.056 |
| | | | | 16 | A.1 | 1 | 0.053 | 4 | C.0 | 3 | 0.019 | 16 | A.1 | 4 | 0.057 |
| 1024 | 0.138 | 0.110 | 0.147 | 32 | C.1 | 4 | 0.040 | 16 | A.0 | 4 | 0.002 | 16 | A.0 | 4 | 0.034 |
| | | | | 32 | A.1 | 2 | 0.043 | **4** | **C.1** | **4** | **0.003** | 64 | A.0 | 4 | 0.036 |
| | | | | 64 | A.0 | 4 | 0.046 | 4 | C.1 | 3 | 0.004 | 32 | A.1 | 4 | 0.038 |
| | (0.093) | (0.120) | (0.111) | 32 | A.1 | 4 | 0.047 | 64 | A.0 | 3 | 0.006 | 64 | A.0 | 3 | 0.038 |
| | | | | 16 | A.1 | 2 | 0.047 | 64 | A.0 | 4 | 0.008 | 32 | C.1 | 4 | 0.039 |
| Av. | 0.154 | 0.135 | 0.170 | 16 | A.1 | 4 | 0.058 | **4** | **C.1** | **4** | **0.004** | **4** | **C.1** | **4** | **0.045** |
| | | | | 16 | A.1 | 1 | 0.058 | 4 | C.1 | 3 | 0.004 | 4 | C.1 | 3 | 0.060 |
| | | | | 16 | A.1 | 3 | 0.059 | 4 | C.0 | 4 | 0.016 | 16 | A.0 | 4 | 0.065 |
| | (0.092) | (0.114) | (0.106) | 32 | C.1 | 4 | 0.060 | 4 | C.0 | 3 | 0.020 | 16 | A.0 | 3 | 0.068 |
| | | | | 16 | A.0 | 3 | 0.061 | 2 | A.1 | 4 | 0.037 | 4 | C.0 | 4 | 0.069 |

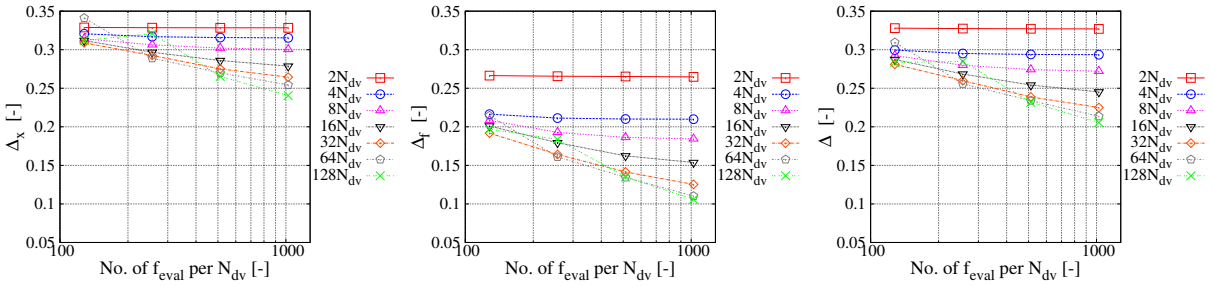


(a) Average performance, conditional to number of particles

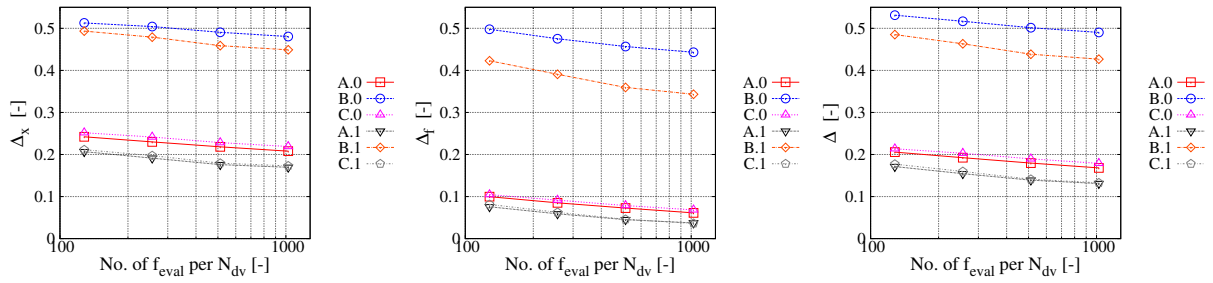


(b) Average performance, conditional to particles initialization

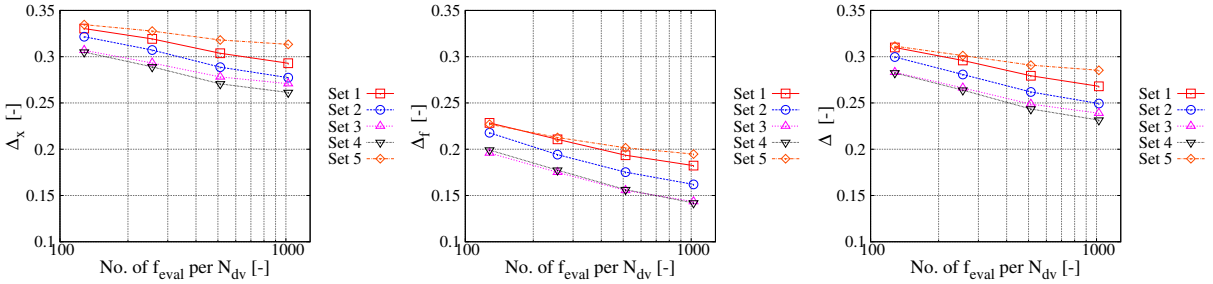


(c) Average performance, conditional to coefficient set

Figure 10: AD-PSO average performance for $N_{dv} \geq 10$

Table 6: Best performing setups for AD-PSO, $N_{dv} \geq 10$

| $N_{feval}/N_{dv}$ | Average (STD) | | | Best AD-PSO | | | | | | | | | | | |
|---|---|---|---|---|---|---|---|---|---|---|---|---|---|---|---|
| | $\Delta_x$ | $\Delta_f$ | $\Delta$ | $\frac{N_p}{N_{dv}}$ | Init | Coef | $\Delta_x$ | $\frac{N_p}{N_{dv}}$ | Init | Coef | $\Delta_f$ | $\frac{N_p}{N_{dv}}$ | Init | Coef | $\Delta$ |
| 128 | 0.320 | 0.214 | 0.297 | 4 | A.1 | 4 | 0.147 | 2 | C.1 | 4 | 0.013 | 4 | A.1 | 4 | 0.107 |
| | | | | 2 | C.1 | 4 | 0.152 | 4 | A.1 | 4 | 0.015 | 2 | C.1 | 4 | 0.109 |
| | | | | 8 | C.1 | 4 | 0.152 | 2 | A.1 | 4 | 0.019 | **4** | **C.1** | **4** | **0.116** |
| | (0.136) | (0.191) | (0.159) | 2 | A.1 | 2 | 0.158 | **4** | **C.1** | **4** | **0.022** | 2 | A.1 | 4 | 0.116 |
| | | | | **4** | **C.1** | **4** | **0.159** | 4 | C.1 | 3 | 0.027 | 8 | C.1 | 4 | 0.117 |
| 256 | 0.307 | 0.194 | 0.282 | 4 | A.1 | 4 | 0.145 | 4 | A.1 | 4 | 0.010 | 4 | A.1 | 4 | 0.104 |
| | | | | 8 | C.1 | 4 | 0.149 | 2 | C.1 | 4 | 0.012 | 8 | C.1 | 4 | 0.108 |
| | | | | 4 | C.1 | 2 | 0.150 | 8 | A.1 | 3 | 0.016 | 2 | C.1 | 4 | 0.108 |
| | (0.137) | (0.190) | (0.160) | 2 | C.1 | 4 | 0.151 | 2 | A.1 | 4 | 0.016 | 4 | C.1 | 2 | 0.111 |
| | | | | 32 | A.1 | 3 | 0.154 | 8 | C.1 | 4 | 0.017 | **4** | **C.1** | **4** | **0.114** |
| 512 | 0.292 | 0.176 | 0.265 | 32 | A.1 | 3 | 0.141 | 16 | A.0 | 3 | 0.010 | 4 | A.1 | 4 | 0.103 |
| | | | | 4 | A.1 | 4 | 0.144 | 4 | A.1 | 4 | 0.010 | 8 | C.1 | 4 | 0.105 |
| | | | | 16 | A.1 | 4 | 0.145 | 8 | A.1 | 4 | 0.011 | 16 | A.1 | 4 | 0.105 |
| | (0.139) | (0.191) | (0.162) | 8 | C.1 | 4 | 0.147 | 2 | C.1 | 4 | 0.012 | 2 | C.1 | 4 | 0.108 |
| | | | | 4 | C.1 | 2 | 0.147 | 16 | A.1 | 4 | 0.013 | 32 | A.1 | 3 | 0.108 |
| 1024 | 0.283 | 0.165 | 0.255 | 32 | A.1 | 3 | 0.136 | 16 | A.1 | 4 | 0.008 | 32 | A.1 | 3 | 0.100 |
| | | | | 64 | C.1 | 3 | 0.140 | 16 | A.0 | 3 | 0.008 | 16 | A.1 | 4 | 0.101 |
| | | | | 128 | A.1 | 2 | 0.141 | 16 | A.0 | 4 | 0.009 | 4 | A.1 | 4 | 0.102 |
| | (0.140) | (0.194) | (0.164) | 32 | C.1 | 4 | 0.142 | 8 | A.1 | 4 | 0.010 | 32 | C.1 | 4 | 0.104 |
| | | | | 16 | A.1 | 4 | 0.142 | 4 | A.1 | 4 | 0.010 | 8 | C.1 | 4 | 0.104 |
| Av. | 0.300 | 0.187 | 0.275 | 4 | A.1 | 4 | 0.145 | 4 | A.1 | 4 | 0.011 | 4 | A.1 | 4 | 0.104 |
| | | | | 8 | C.1 | 4 | 0.148 | 2 | C.1 | 4 | 0.012 | 2 | C.1 | 4 | 0.108 |
| | | | | 2 | C.1 | 4 | 0.151 | 2 | A.1 | 4 | 0.016 | 8 | C.1 | 4 | 0.108 |
| | (0.136) | (0.190) | (0.160) | 4 | C.1 | 2 | 0.151 | **4** | **C.1** | **4** | **0.018** | 4 | C.1 | 2 | 0.112 |
| | | | | 32 | A.1 | 3 | 0.152 | 8 | A.1 | 3 | 0.018 | **4** | **C.1** | **4** | **0.114** |

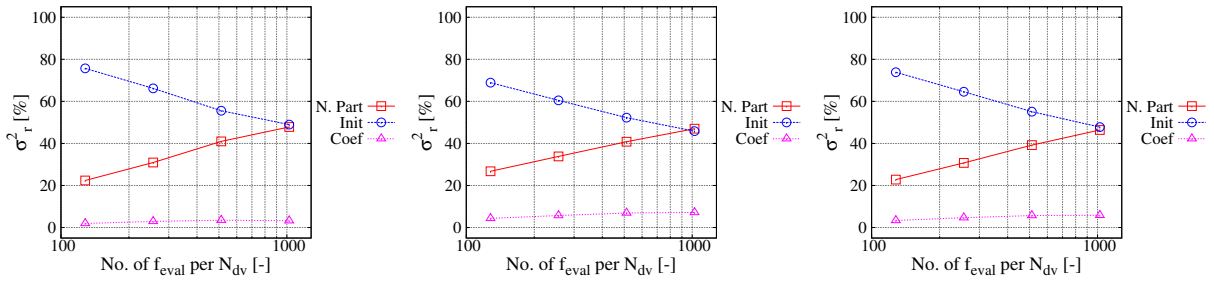


(a) $\Delta_x$ (b) $\Delta_f$ (c) $\Delta$

Figure 11: $\sigma_r^2(\%)$ of AD-PSO for $N_{dv} < 10$

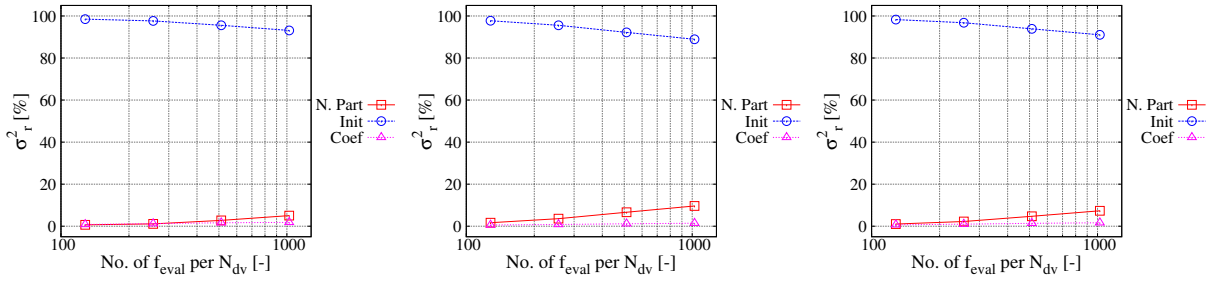


(a) $\Delta_x$ (b) $\Delta_f$ (c) $\Delta$

Figure 12: $\sigma_r^2(\%)$ of AD-PSO for $N_{dv} \geq 10$

### 5.1.3 Suggested guideline for S/A D-PSO

The most frequent setup is selected in Tabs. 3, 4, 5 and 6, in order to define a guideline for the use of S/A D-PSO as simple and general as possible. This corresponds to a number of particles $N_p$ equal to $4$ times the number of design variables $N_{dv}$, a particles initialization including distribution on domain and bounds with non-null velocity, and the set of coefficients by Clerc (2006) [18], $\chi = 0.721$, $c_1 = c_2 = 1.655$. The guideline is summarized in Tab. 7.

Table 7: Suggested guideline for S/A D-PSO

| $N_p/N_{dv}$ | Init | Coef |
|---|---|---|
| 4 | C.1 (including domain and bounds) | 4 (Clerc, 2006) |

Figures 13 and 14 show the performance of the suggested PSO setup, for SD-PSO and AD-PSO and $N_{dv} < 10$ and $\geq 10$, respectively. Average performance, standard deviation and best performing setup among all combinations is shown for each budget. The guideline setup is found always very close or coincident to the best. In addition, it may be noted how AD-PSO is always equivalent or slightly better than SD-PSO.

## 5.2 High-speed catamaran SBD optimization

A preliminary sensitivity analysis for each design variable is shown in Fig. 15, showing $\Delta_{obj}$ compared to the parent hull. Changes in $\Delta_{obj}$ are found significant in each direction, revealing a reduction of the objective function close to $9\%$ for the $4D$ design space, and close to $10\%$ for the $6D$.

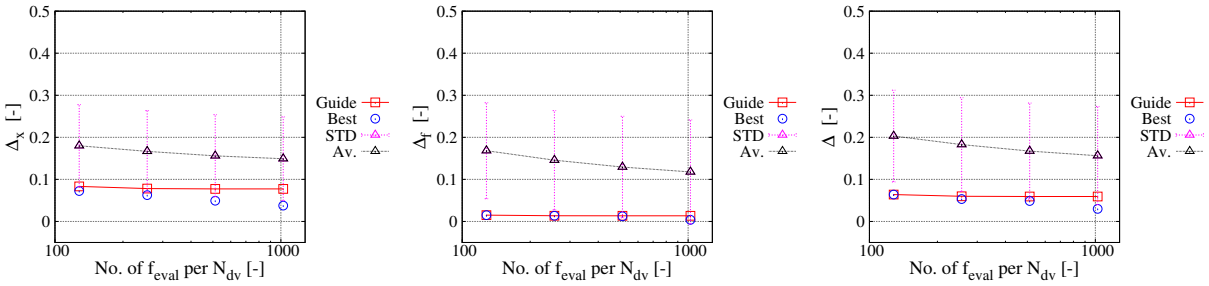


(a) $N_{dv} < 10$

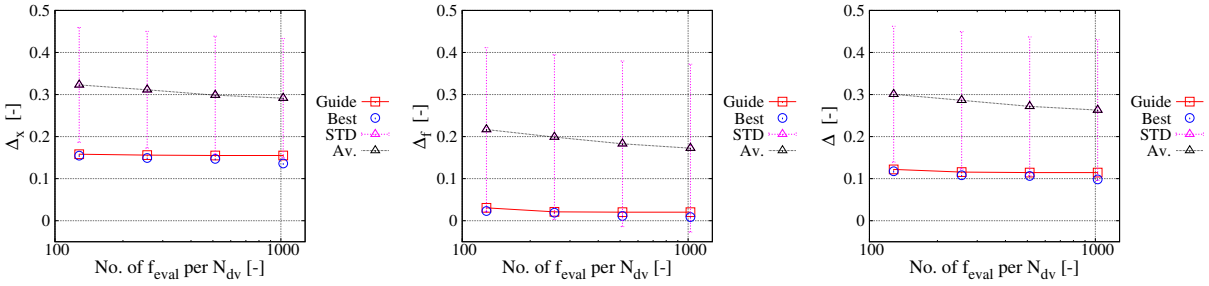


(b) $N_{dv} \geq 10$

Figure 13: Performance of suggested guideline using SD-PSO

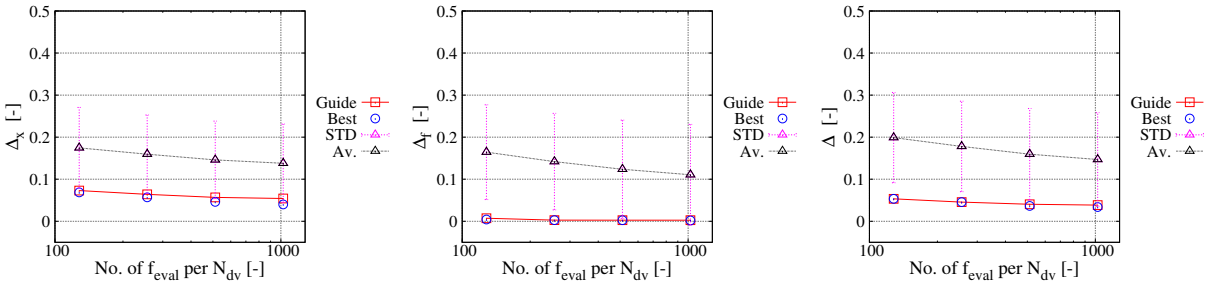


(a) $N_{dv} < 10$

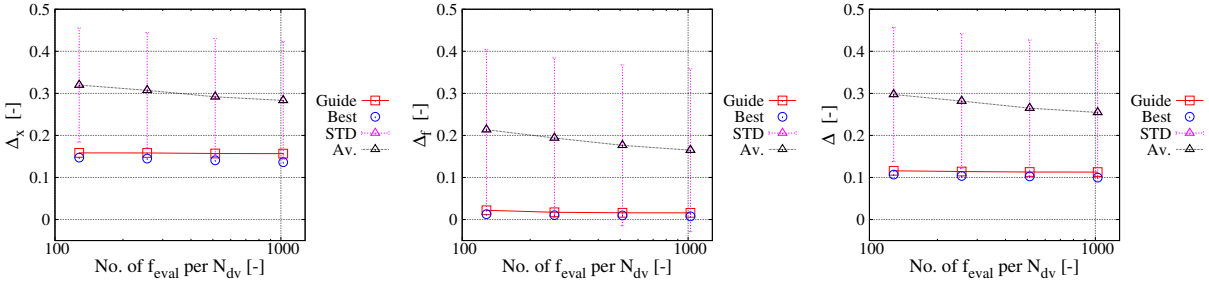


(b) $N_{dv} \geq 10$

Figure 14: Performance of suggested guideline using AD-PSO

Optimization results in Tab. 8 show that both algorithms (S/A D-PSO) with IW and SEW lead to a reduction of the objective function close to $20\%$ for the $4D$ design space and greater than $20\%$ for the $6D$ design space. Furthermore the optimum configuration leads to a considerable reduction of wave's elevation compared to the original geometry (Figs. 17 and 18). There are not significant differences between the results obtained by SD-PSO and AD-PSO except for SD-PSO with IW for the $6D$ design space. In this case the optimization stops after 6 PSO

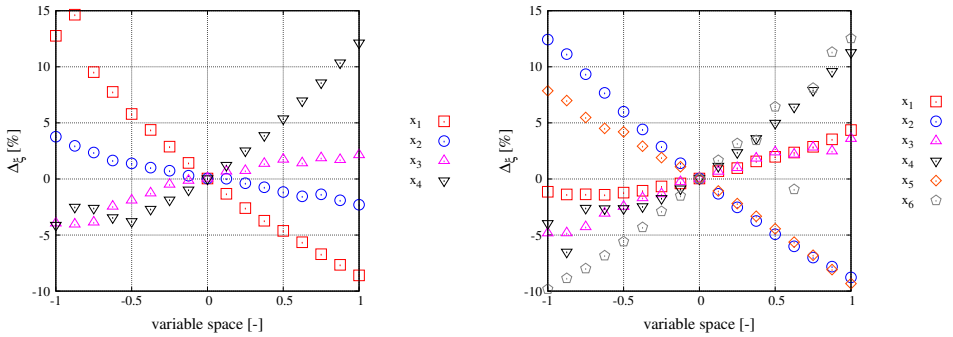


(a) $4D$ design space (b) $6D$ design space

Figure 15: Sensitivity analysis

iterations, due to IW approach. As shown in Fig. 16, differences in optimal design variables are due to the use of IW or SEW for box constraints. The final configuration for the first design space ($4D$) is fairly close (except for the second variable) to that obtained using metamodels with a URANS solver [4] (Fig. 16a), while for the second design space ($6D$) the differences are more significant (Fig. 16b). Finally, S/A D-PSO iterations are shown in Fig. 19, revealing a quite sudden convergence.

Table 8: SBD results

| Design space | | wall approach | $R_t$ [N] | $\delta$ [N] | $obj$ | $\Delta_{obj}(\%)$ |
|---|---|---|---|---|---|---|
| | Original | | 50.15 | 852.5 | 5.88e-2 | |
| $4D$ | SD-PSO | IW | 39.92 | 850.9 | 4.69e-2 | -20.24 |
| | | SEW | 40.36 | 850.6 | 4.67e-2 | -20.57 |
| | AD-PSO | IW | 39.85 | 851.1 | 4.68e-2 | -20.41 |
| | | SEW | 40.68 | 851.7 | 4.71e-2 | -19.90 |
| $6D$ | SD-PSO | IW | 39.41 | 849.1 | 4.64e-2 | -21.10 |
| | | SEW | 34.29 | 835.4 | 4.10e-2 | -30.27 |
| | AD-PSO | IW | 34.31 | 835.5 | 4.11e-2 | -30.10 |
| | | SEW | 34.08 | 830.8 | 4.09e-2 | -30.30 |

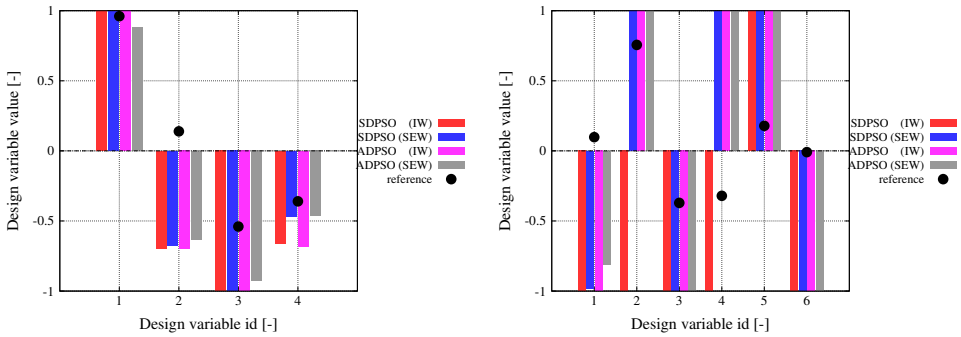


(a) $4D$ design space (b) $6D$ design space

Figure 16: Comparison between optimal design variables of SD-PSO, AD-PSO with IW and SEW by PF and those obtained by metamodels with URANS in [4]

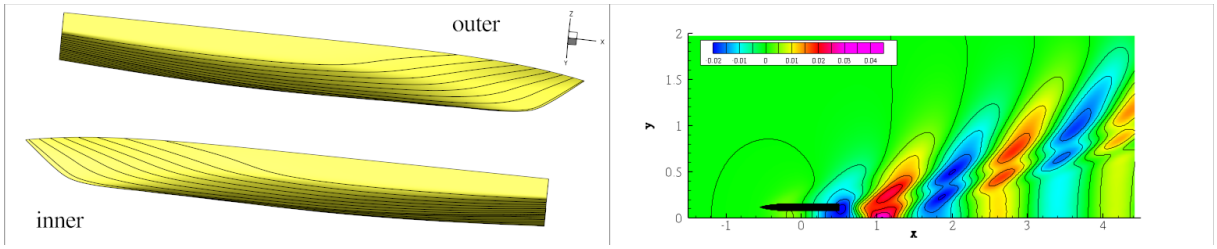


(a) Original Delft catamaran

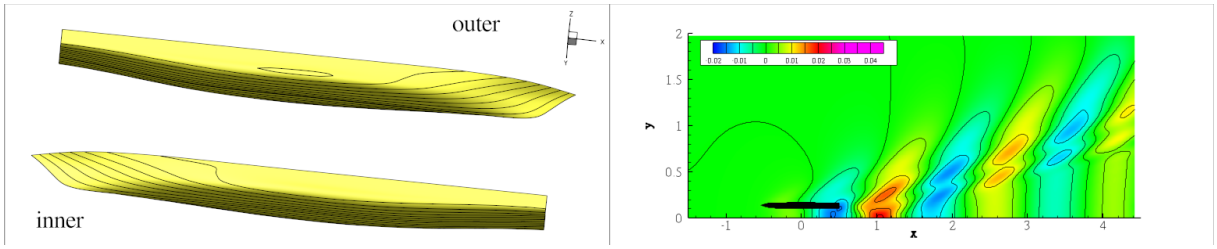


(b) SD-PSO with IW

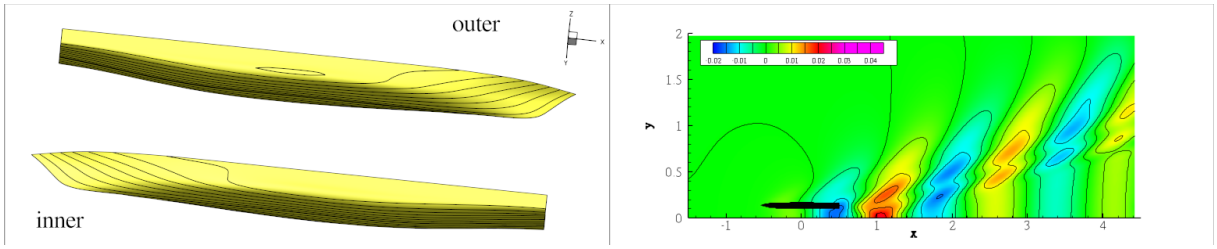


(c) SD-PSO with SEW

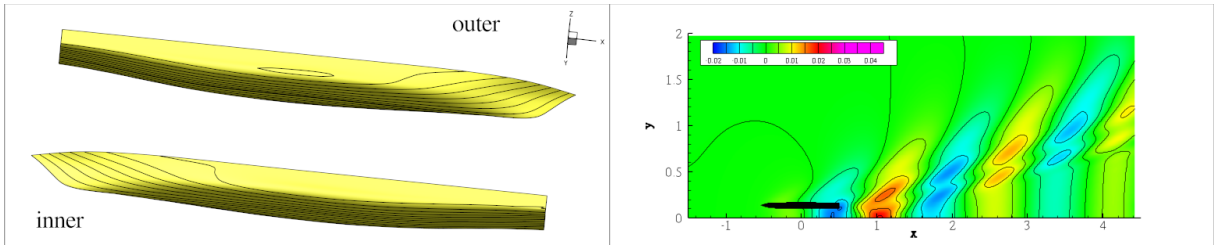


(d) AD-PSO with IW

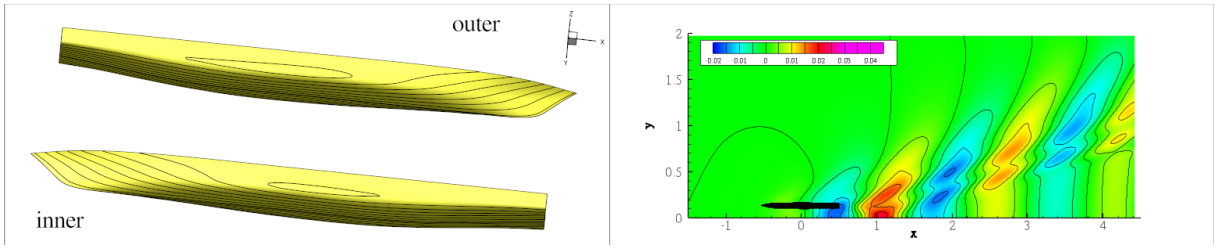


(e) AD-PSO with SEW

Figure 17: $4D$ SBD results

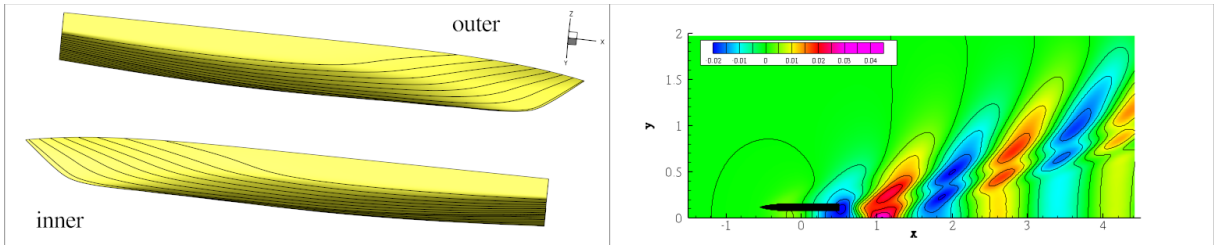


(a) Original Delft catamaran

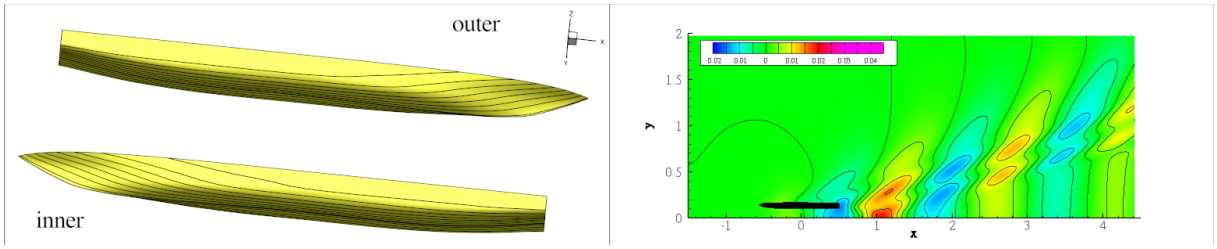


(b) SD-PSO with IW

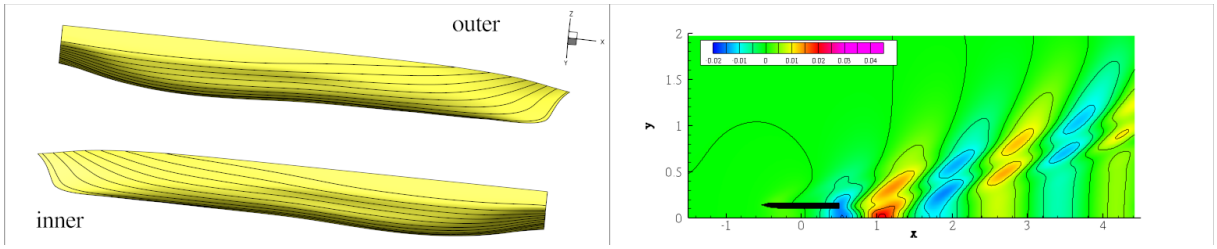


(c) SD-PSO with SEW

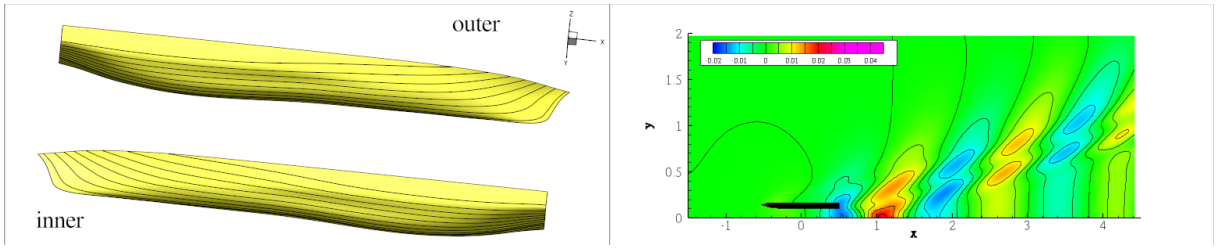


(d) AD-PSO with IW

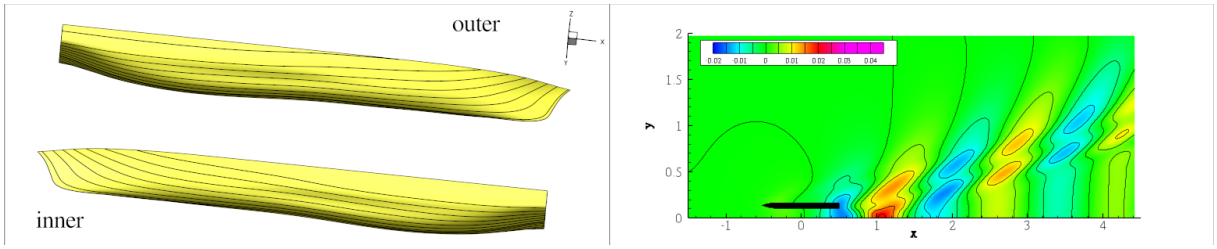


(e) AD-PSO with SEW

Figure 18: $6D$ SBD results

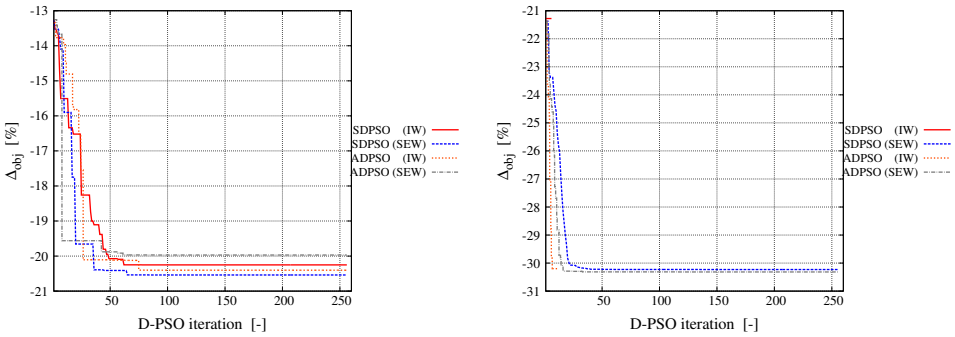


(a) $4D$ design space (b) $6D$ design space

Figure 19: Convergence of S/A D-PSO

## 6 CONCLUSIONS AND FUTURE WORK

A guideline for an effective and efficient use of S/A D-PSO has been suggested and discussed, assuming limited computational resources. A parametric analysis has been conducted using 60 analytical test functions from literature and three different absolute performance criteria, varying the number of particles, the initialization of the swarm, and the set of coefficients. All possible combinations of PSO parameters led to 210 optimizations for each function. The most promising PSO setup has been identified and successfully applied to a ship SBD optimization problem, namely the high-speed Delft catamaran advancing in calm water at fixed speed using a potential-flow code. The optimization pertained to the hull form and aimed at the total resistance over displacement ratio reduction, using four- and six-dimensional design spaces.

The outcomes of the current analysis may be summarized as follows:

- The particles initialization has been found the most significant PSO parameter, especially for $N_{dv} \geq 10$ and low budgets of function evaluations. Conversely, the coefficient set has been found with a little influence on the PSO performance, compared to other parameters.
- The suggested guideline setup corresponds to: a number of particles $N_p$ equal to $4$ times the number of design variables $N_{dv}$; particles initialization including (Hammersley) distribution on domain and bounds with non-null velocity; set of coefficient by Clerc (2006) [18], i.e., $\chi = 0.721$, $c_1 = c_2 = 1.655$.
- The guideline setup has been found always very close or coincident to the best setup among all 210 available, for each budget. In addition, it has been proven to perform well for a $4D$ and a $6D$ ship SBD problems.
- AD-PSO has been found with equivalent performance to SD-PSO.
- SEW approach for box constraints should be preferred to IW, in order to avoid an early arrest of the swarm particles.

Future work includes developments for new particles initialization methodologies, with application to test functions and ship SBD problems, using S/A D-PSO. Future research also includes the extension of present studies to multi-objective D-PSO with application to reliability-based robust design optimization [30].

## ACKNOWLEDGEMENTS

The present research is supported by the US Office of Naval Research, NICOP Grant N62909-11-1-7011, under the administration of Dr. Ki-Han Kim and Dr. Woei-Min Lin, and by the Italian Flagship Project RITMARE, coordinated by the Italian National Research Council and funded by the Italian Ministry of Education, within the National Research Program 2011-2013.

## REFERENCES

[1] J. Kennedy, R.C. Eberhart, Particle swarm optimization, in: *Proc. IEEE Conf. on Neural Networks, IV*, Piscataway, NJ, 1995, pp. 1942-1948.

[2] R.C. Eberhart, J. Kennedy, A new optimizer using particle swarm theory, *Proc. Sixth Intl. Symp. on Micro Machine and Human Science (Nagoja, Japan)*, IEEE Service Center, Piscantaway, NJ, 1995, pp. 39-43.

[3] E.F. Campana, G. Liuzzi, S. Lucidi, D. Peri, V. Piccialli, A. Pinto, New global optimization methods for ship design problems, *Optimization and Engineering*, December 2009, Volume 10, Issue 4, pp. 533-555.

[4] X. Chen, M. Diez, M. Kandasamy, Z. Zhang, E.F. Campana, F. Stern, High-fidelity global optimization for shape design by dimensionality reduction, metamodels and deterministic particle swarm, *Engineering Optimization*, 2014.

[5] G. Venter, J. Sobieszczanski-Sobieski, A parallel particle swarm optimization algorithm accelerated by asynchronous evaluations, *6th World Congresses of Structural and Multidisciplinary Optimization*, Rio de Janeiro, 30 May–03 June 2005, Brazil.

[6] B.-I. Koh, A.D. George, R.T. Haftka, B.J. Fregly, Parallel asynchronous particle swarm optimization, *Int. J. Numer. Meth. Engng* 2006; 67:578–595, DOI: 10.1002/nme.1646.

[7] M. Kandasamy, D. Peri, Y. Tahara, W. Wilson, M. Miozzi, S. Georgiev, E. Milanov, E.F. Campana, F. Stern, Simulation based design optimization of waterjet propelled Delft catamaran, *International Shipbuilding Progress*, Volume 60, 2013, pp. 277-308, DOI 10.3233/ISP-130098.

[8] X. Chen, M. Diez, M. Kandasamy, E.F. Campana, F. Stern, Design optimization of the waterjet-propelled Delft Catamaran in calm water using URANS, design of experiments, metamodels and swarm intelligence, *12th International Conference on Fast Sea Transportation*, FAST2013, Amsterdam, The Netherlands, 2013.

[9] B. Rosenthal, D.C. Kring, Optimal design of a lifting body SWATH, *12th International Conference on Fast Sea Transportation*, FAST2013, Amsterdam, The Netherlands, 2013.

[10] R. Poli, J. Kennedy, T. Blackwell, Particle Swarm Optimization - An overview, *Swarm Intell*, 2007, Volume 1, pp. 33-57.

[11] S. Lucidi, M. Piccioni, Random Tunneling by Means of Acceptance-Rejection Sampling for Global Optimization, *Journal of optimization theory and applications*, Vol. 62, N. 2, August 1989, pp. 255-277.

[12] E.F. Campana, G. Fasano, A. Pinto, Dynamic analysis for the selection of parameters and initial population, in particle swarm optimization, *Journal of Global Optimization*, November 2010, Volume 48, Issue 3, pp. 347-397.

[13] T.T. Wong, W.S. Luk, P.A. Heng, Sampling with Hammersley and Halton Points, *Journal of Graphics Tools*, 1997, pp. 9-24.

[14] Y. Shi, R.C. Eberhart, Parameter selection in particle swarm optimization, *Proceedings of Evolutionary Programming VII (EP98)*, 1998, pp. 591-600.

[15] M. Clerc, J. Kennedy, The particle swarm: explosion, stability and convergence in a multi-dimensional complex space, *IEEE Trans Evolution. Comput.* 6(1), 2002, pp. 58-73.

[16] A. Carlisle, G. Dozier, An Off-the-shelf PSO, *Proceding of the Workshop on Particle Swarm Optimization*, 2001, pp. 1-6.

[17] I.C. Trelea, The particle swarm optimization algorithm: convergence analysis and parameter selection, *Information Processing Letters*, 85, 2003, pp. 317-325.

[18] M. Clerc, Stagnation analysis in particle swarm optimization or what happens when nothing happens, *http://hal.archives-ouvertes.fr/hal-00122031*, Tech. Rep. 2006.

[19] D. Peri, F. Tinti, A multistart gradient-based algorithm with surrogate model for global optimization, *Communications in Applied and Industrial Mathematics*, 2012.

[20] S. Helwig, J. Branke, S. Mostaghim, Experimental Analysis of Bound Handling Techniques in Particle Swarm Optimization, *IEEE Transactions on Evolutionary computation*, Vol. 17, No. 2, April 2013.

[21] P. Bassanini, U. Bulgarelli, E.F. Campana, F. Lalli, The wave resistance problem in a boundary integral formulation, *Surv. Math. Ind.* (1994) 4:151-194.

[22] Y. Shi, R.C. Eberhart, A modified Particle Swarm Optimizer, *IEEE International Conference on Evolutionary Computation*, Anchorage, Alaska, 1998.

[23] M. Clerc, The swarm and the queen: towards a deterministic and adaptive particle swarm optimization, in: *Proc. ICEC*, Washington, DC, 1999, pp. 1951-1957.

[24] R.C Eberhart, Y. Shi, Comparing inertia weights and constriction factor in particle swarm optimization, in *Congress on Evolutionary Computing*, vol. 1, pp. 84–88, 2000.

[25] R.C. Eberhart, Y. Shi, Particle Swarm Optimization: Developments, Applications and Resources, *Evolutionary computation*, 2001.

[26] M. Clerc, Confinements and Biases in Particle Swarm Optimization, *http://clerc.maurice.free.fr/pso*, 2006.

[27] D. Bratton, J. Kennedy, Defining a standard for particle swarm optimization, in *Proc. IEEE Swarm Intell. Symp*, Apr. 2007, pp. 120-127.

[28] A. Levy, A. Montalvo, S. Gomez, and A. Galderon, Topics in Global Optimization, *Lecture Notes in Mathematics No. 909*, Springer-Verlag, 1981.

[29] H. Schlichting, K. Gersten, *Boundary-Layer Theory*, Springer-Verlag, Berlin, 2000.

[30] M. Diez, X. Chen, E.F. Campana, F. Stern, *Reliability-based robust design optimization for ships in real ocean evironment*, 12th International Conference on Fast Sea Transportation FAST2013, Amsterdam, December 2013.

## A LIST OF TEST FUNCTIONS

Table 9 summarizes the test functions used in the current work.

Table 9: Test functions

| $f_k(\mathbf{x})$ | **Name** | **Dimension** $N_{dv}$ | **Bounds** $[x_{min}, x_{max}]^{i,\dots,N_{dv}}$ | **Optimum** $\min\ f(\mathbf{x})$ |
|---|---|---|---|---|
| $f_1(x)$ | Sphere | 2 | $[-5,5]^{N_{dv}}$ | 0.000 |
| $f_2(x)$ | Freudenstein-Roth | 2 | $[-5,5]^{N_{dv}}$ | 0.000 |
| $f_3(x)$ | Ackley | 2 | $[-5,5]^{N_{dv}}$ | 0.000 |
| $f_4(x)$ | Three-Hump Camel Back | 2 | $[-5,5]^{N_{dv}}$ | 0.000 |
| $f_5(x)$ | Six-Hump Camel Back | 2 | $[-2.5,2.5]^{i}$, $[-1.5,1.5]^{j}$ | -1.032 |
| $f_6(x)$ | Quartic | 2 | $[-10,10]^{N_{dv}}$ | -0.352 |
| $f_7(x)$ | Beale | 2 | $[-4.5,4.5]^{N_{dv}}$ | 0.000 |
| $f_8(x)$ | Schubert penalty 1 | 2 | $[-10,10]^{N_{dv}}$ | -186.731 |
| $f_9(x)$ | Schubert penalty 2 | 2 | $[-10,10]^{N_{dv}}$ | -186.731 |
| $f_{10}(x)$ | Booth | 2 | $[-10,10]^{N_{dv}}$ | 0.000 |
| $f_{11}(x)$ | Matyas | 2 | $[-10,10]^{N_{dv}}$ | 0.000 |
| $f_{12}(x)$ | Goldstein-Price | 2 | $[-2,2]^{N_{dv}}$ | 3.000 |
| $f_{13}(x)$ | Bukin n.6 | 2 | $[-15,-5]^{i}$, $[-3,3]^{j}$ | 0.000 |
| $f_{14}(x)$ | Rosenbrock | 2 | $[-100,100]^{N_{dv}}$ | 0.000 |
| $f_{15}(x)$ | Schaffer n.2 | 2 | $[-100,100]^{N_{dv}}$ | 0.000 |
| $f_{16}(x)$ | Schaffer n.6 | 2 | $[-100,100]^{N_{dv}}$ | 0.000 |
| $f_{17}(x)$ | Easom | 2 | $[-100,100]^{N_{dv}}$ | -1.000 |
| $f_{18}(x)$ | Test Tube Holder | 2 | $[-10,10]^{N_{dv}}$ | -10.872 |
| $f_{19}(x)$ | Treccani | 2 | $[-5,5]^{N_{dv}}$ | 0.000 |
| $f_{20}(x)$ | Tripod | 2 | $[-100,100]^{N_{dv}}$ | 0.000 |
| $f_{21,22}(x)$ | Exponential | 2, 4 | $[-10,10]^{N_{dv}}$ | -1.000 |
| $f_{23,24}(x)$ | Styblinski-Tang | 2, 4 | $[-5,5]^{N_{dv}}$ | $-39.166 \cdot N_{dv}$ |
| $f_{25,26}(x)$ | Cosine Mixture | 2, 4 | $[-1,1]^{N_{dv}}$ | $-0.100 \cdot N_{dv}$ |
| $f_{27,28}(x)$ | Hartman n.3, n.6 | 3, 6 | $[0,1]^{N_{dv}}$ | -3.860, -3.320 |
| $f_{29,30,31,32}(x)$ | $5^n$ loc. minima (Levy) | 2, 5, 10, 20 | $[-10,10]^{N_{dv}}$ | 0.000 |
| $f_{33,34,35,36}(x)$ | $10^n$ loc. minima (Levy) | 2, 5, 10, 20 | $[-10,10]^{N_{dv}}$ | 0.000 |
| $f_{37,38,39,40}(x)$ | $15^n$ loc. minima (Levy) | 2, 5, 10, 20 | $[-5,5]^{N_{dv}}$ | 0.000 |
| $f_{41,42,43,44}(x)$ | Griewank | 2, 5, 10, 20 | $[-10,10]^{N_{dv}}$ | 0.000 |
| $f_{45,46,47,48}(x)$ | Alpine | 2, 5, 10, 20 | $[-10,10]^{N_{dv}}$ | 0.000 |
| $f_{49,50,51,52}(x)$ | Multi Modal | 2, 5, 10, 20 | $[-10,10]^{N_{dv}}$ | 0.000 |
| $f_{53,54,55,56}(x)$ | Dixon-Price | 2, 5, 10, 20 | $[-10,10]^{N_{dv}}$ | 0.000 |
| $f_{57}(x)$ | Colville | 4 | $[-10,10]^{N_{dv}}$ | 0.000 |
| $f_{58}(x)$ | Shekel n.5 | 4 | $[0,10]^{N_{dv}}$ | -10.153 |
| $f_{59}(x)$ | Shekel n.7 | 4 | $[0,10]^{N_{dv}}$ | -10.403 |
| $f_{60}(x)$ | Shekel n.10 | 4 | $[0,10]^{N_{dv}}$ | -10.536 |